CHEMICAL ENGINEERING TRANSACTIONS
VOL. 94, 2022
A publication of AIDIC
The Italian Association of Chemical Engineering
Online at www.cetjournal.it
Guest Editors: Petar S. Varbanov, Yee Van Fan, Jiří J. Klemeš, Sandro Nižetić

ISBN 978-88-95608-93-8; **ISSN** 2283-9216
DOI: 10.3303/CET2294025

Evaluation of Magnesium-Based Primary Battery for Powering Transient Electronics

Justine Marie E. Abarro[a], Joey D. Ocon[a,b], Julie Anne D. del Rosario[a,b,*]

[a]Laboratory of Electrochemical Engineering (LEE), Department of Chemical Engineering, University of the Philippines Diliman, Quezon City 1101, Philippines
[b]Energy Engineering Program, National Graduate School of Engineering, College of Engineering, University of the Philippines Diliman, Quezon City 1101, Philippines
jddelrosario2@up.edu.ph

A new class of technology known as transient electronics has the potential to reduce electronic waste with its unique ability to dissolve under a specific condition. Biodegradable batteries are essential to realizing fully integrated and self-sufficient systems. Pure magnesium-based materials are among the widely explored transient electrodes due to their superior mechanical properties. However, such materials have rapid degradation rates. AZ31, an alloy of Mg containing 3 % aluminum (Al) and 1 % zinc (Zn) by weight, has more stable corrosion product layers, making them advantageous as anode materials. In this work, the electrochemical performance of the two full cell combinations of Mg and AZ31 anodes each paired with copper oxide (CuO) cathode were compared in a seawater electrolyte. To produce the cathodes, pristine copper foils were galvanostatically anodized at a current density of 2.0 mA/cm^2 for 90 min. Results showed that AZ31-based cell has a higher specific energy of 1.63 J/cm^2 compared to pure Mg-based cell which has 1.08 J/cm^2. The observed nominal operating voltages for an AZ31-based cell were 1.1 V for the first 0.6 h and remained at 0.8 V for the next 5.6 h when discharged at a current density of 0.25 mA/cm^2. The AZ31-based cell also yields a better specific capacity of 2.17 mAh/cm^2 and a discharge time of 8.68 h, which is twice the capacity and the discharge life of a pure Mg-based cell. The reported increase in performance is attributed to the presence of alloying components in the anode which limits the parasitic corrosion inherent in a pure Mg anode.

1. Introduction

The fundamental goal in developing a novel class of electronics is to achieve high power performance and stable operation. The emergence of biodegradable technology offers innovative solutions that non-degradable electronics cannot achieve. For instance, transient electronics have the unique ability to partially or completely disintegrate in a controlled manner (Hwang et al., 2012). This green technology allows for extensive applications, especially in environmental sensing and monitoring while potentially minimizing electronic wastes. However, the existing energy sources for transient devices are external-based such as inductive coupling in short-range distances and other external power supplies (Hwang et al., 2013). In this respect, energy source has been limited to passive designs or wireless power, to which energy transfer is affected by several external factors (Chen et al., 2010).

Recent progress in transient batteries has several shortcomings such as the low operational voltage, power density, stability, and operational time which are mainly attributed to the electrode material (Chen et al., 2016). Magnesium is a widely studied anode for transient batteries because of its high energy density and desirable biocompatibility (Yin et al., 2014). However, Mg is aggressively susceptible to pitting corrosion, especially in an aqueous marine environment (Tsang et al., 2015). To prevent parasitic corrosion, this study optimized the anode material by considering magnesium alloy AZ31 (3 % aluminum, 1 % zinc). AZ31 was reported to have improved ultimate tensile strength of ~230 MPa compared to that of pure Mg (~90 MPa) (Li et al., 2014). The presence of Al forms an intermetallic β-phase with Mg while fine-grain Zn situates at grain boundary defects (Acharya and Shetty, 2019).

Paper Received: 15 April 2022; Revised: 28 June 2022; Accepted: 05 July 2022
Please cite this article as: Abarro J.M.E., Ocon J.D., Del Rosario J.A.D., 2022, Evaluation of Magnesium-Based Primary Battery for Powering Transient Electronics, Chemical Engineering Transactions, 94, 151-156 DOI:10.3303/CET2294025

To produce high-power transient batteries, it is imperative to select a compatible cathode that would give stable voltage curves during operation. Cu was regarded as a biodegradable metal with excellent electrical conductivity but degrades in solutions with high chloride concentration (Tao et al., 2007). Xiao et al. (2015) formed a nanoneedle array film on the Cu surface through controlled anodization to create an anticorrosion protection. Togonon et al. (2021) also reported that the metal oxides synthesized via anodization enabled additional sites for hydrogen evolution reaction which increased the operating voltages of the battery. Currently, there is a lack of available studies that evaluate the performance of AZ31-CuO cell combination in chloride-containing media. Thus, this work evaluated the alloying effects of AZ31-CuO cell combination and compared its electrochemical performance with pure Mg-CuO in a seawater electrolyte.

2. Methodology

The methodology of the study is divided into sections—material preparation, galvanostatic anodization of the copper cathode, surface characterization of the anodized copper, and the electrochemical measurements of the full cell to evaluate its behavior in seawater with simple nutrients.

2.1 Material preparation

Commercially available Mg (Goodfellow Cambridge Ltd., 99.99 %, 25 mm x 25 mm), AZ31 (96 % Mg, 3 % Al, 1 % Zn, 25 mm x 25 mm), and Cu (99.99 %, 50 mm x 50 mm) metal foils were used as the electrode materials. The metal foils were cut to strips (5 mm x 25 mm), then quickly cleaned using a minimal amount of 0.01 M HCl (Sigma-Aldrich) to remove the local oxides present on the metal surface. The electrolyte used was a seawater with simple nutrients (QC3179, certified reference material) purchased from Sigma-Aldrich; concerning nutrients present also include nitrate, nitrite, ammonia, and orthophosphate. No further testing was conducted on the electrolyte to determine the specific composition, but a certificate of analysis provided by the supplier was made the reference instead.

2.2 Cu anodization

Pristine Cu foil was galvanostatically discharged through a potentiostat (Metrohm Autolab PGSTAT302N). A three-electrode configuration was implemented with the metal sample as the working electrode, saturated silver/silver chloride (Ag/AgCl) as the reference electrode, and a platinum (Pt) mesh as the counter electrode. A portion of 5 mm x 15 mm of the Cu strip was submerged in a 2.0 M KOH solution, and the remaining portion was used as the electrical contact. A constant current density of 2.0 mA/cm^2 was applied for 90 min. Based on the work of Togonon et al. (2021), this method allows for a sufficient and uniform growth oxide layer on the surface of the metal foil.

2.3 Cu anode characterization

To understand the surface morphology of the anodized Cu foil, a scanning electron microscope (FEI Quanta FEG) was used to validate the uniformity of the surface. Different sites were evaluated at varying magnification to determine the surface morphology and confirm the uniformity of the oxide layer produced.

2.4 Electrochemical measurements

The current-voltage (I-V) curves, discharge profile, and corrosion activity of the two full cells were evaluated.

2.4.1 Current-voltage curves

Electrode combinations of Mg and AZ31 anodes paired with anodized Cu as the cathode were characterized by performing galvanostatic discharge tests in seawater electrolyte using a potentiostat (Metrohm Autolab PGSTAT302N) in a two-electrode configuration. The submerged section of the cell has a surface area of 15mm x 5mm. This portion is the electrochemically active area that reacts with the electrolyte. Constant current densities ranging from 0.05 mA/cm^2 to 1 mA/cm^2 with 0.05 mA/cm^2 increment for 150 s were applied to obtain the I-V curve.

2.4.2 Discharge test

The galvanostatic discharge testing was performed using a potentiostat in a two-electrode-cell configuration in a 50 mL seawater electrolyte until the materials degrade. The different cells were discharged at a constant current density of 0.25 mA/cm^2. The performance of different cells was also evaluated at higher current densities

of 0.50 mA/cm^2 and 0.75 mA/cm^2 to determine the behavior. From the I-V curve, the corresponding specific power (P) can be calculated from the product of operating potential (V) and discharge current (I).

2.4.3 Corrosion test

The corrosion test was performed using a potentiostat in a three-electrode-cell configuration with the anode samples as the working electrode, saturated silver/silver chloride (Ag/AgCl) as the reference electrode, and a platinum (Pt) mesh as the counter electrodes. The samples were immersed in the seawater solution for 5 min to allow equilibrium upon testing.

3. Results and discussion

Galvanostatic anodization is an economical and facile method to produce self-deployed nanostructures over a vast surface area. This process is scalable and has the advantage of precise distribution of oxide layer. The anodic layer is considered to be stronger and more adherent than other forms of oxide layer produced from chemical etching (Edupuganti and Solanki, 2016). The anodic Cu films produced a stable thorn-like structures. Anodization period has a clear effect on the quality of the anode produced when the duration was varied from 30 min, 60 min, and 90 min. The latter showed dense and good distribution of oxide layer over the surface.

3.1 Current-voltage curves

The difference between the standard reduction potential of two metal electrodes is the theoretical basis to estimate the operating voltages of a cell. On the other hand, cell voltage is determined to be the difference between the two electrode reduction potentials. Togonon et al. (2021) suggested that two possible reactions at the cathode can either be the reduction of oxygen or the evolution of hydrogen, while magnesium is oxidized at the anode. According to Yun et al. (2009), the main electrochemical reactions involved are:

$Mg \rightarrow Mg^{2+} + 2e^-$	E^o = -2.34 V	(anodic reaction)	(1)
$2H_2O + 2e^- \rightarrow H_2 + 2OH^-$	E^o = -0.83 V	(cathodic reaction)	(2)
$2H_2O + O_2 + 4e^- \rightarrow 4OH^-$	E^o = +0.40 V	(cathodic reaction)	(3)
$Mg^{2+} + 2OH \rightarrow Mg(OH)_2$	E^o = 1.51 V / E^o = -2.74 V	(product formation)	(4)

Figure 1 shows the I-V characteristic curves of the two battery chemistries. Mg-based cells show slightly higher working potential than its alloy counterpart as the current density is increased. At lower discharge current densities (<0.6 mA/cm^2), AZ31 cells have an operating voltage of about 1.0 V.

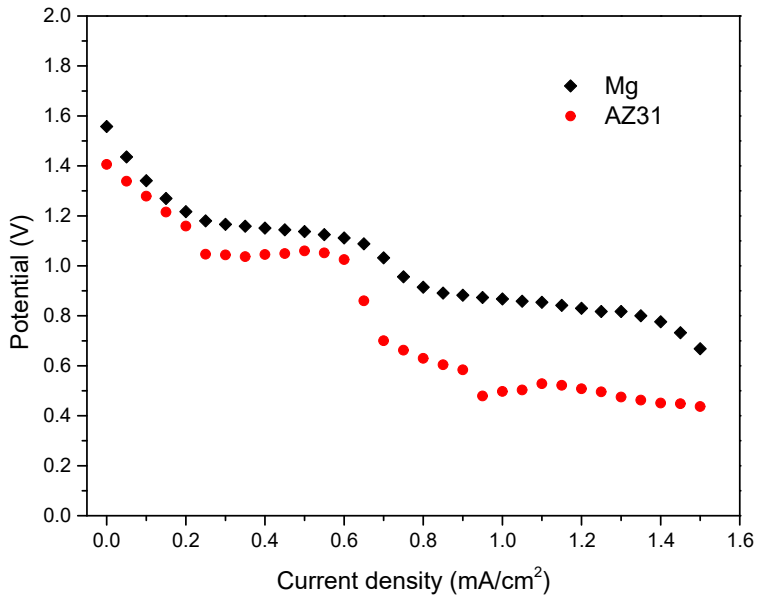

Figure 1: Current-voltage curves of Mg and AZ31-based cells in seawater when constant current densities ranging from 0.05 mA/cm^2 to 1 mA/cm^2 are applied for 150 s at each 0.05 mA/cm^2 increment.

When relatively high discharge rate is applied, the working potential significantly drops. The high working voltage observed at low discharge current densities are caused by the dominance of oxidation reduction. Otherwise, hydrogen evolution reaction becomes the cathodic reaction. With the large voltage difference from the theoretical, hydrogen gas forming at the cathode decreased the cell voltage and the corrosive $Mg(OH)_2$ species accumulating at the electrode-electrolyte boundary increased the cell resistance (Edupuganti and Solanki, 2016).

3.2 Discharge profile

A galvanostatic discharge test can evaluate the capacity and kinetic behavior of the cells. The discharge profile of both cell combinations in Figure 2 shows observable fluctuations that may be attributed to electrode interaction with the solution. Seawater is a conductive, aqueous solution composed of dissolved salts and chlorine, sulfide, and phosphate ions which may form less soluble compounds with Mg. The formation of $Mg(OH)_2$ during discharge leads to accumulation on the electrode-electrolyte interphase to form the passivation layer (Xin et al., 2007). This polarization effect can also be observed with the high losses in the nominal voltage.

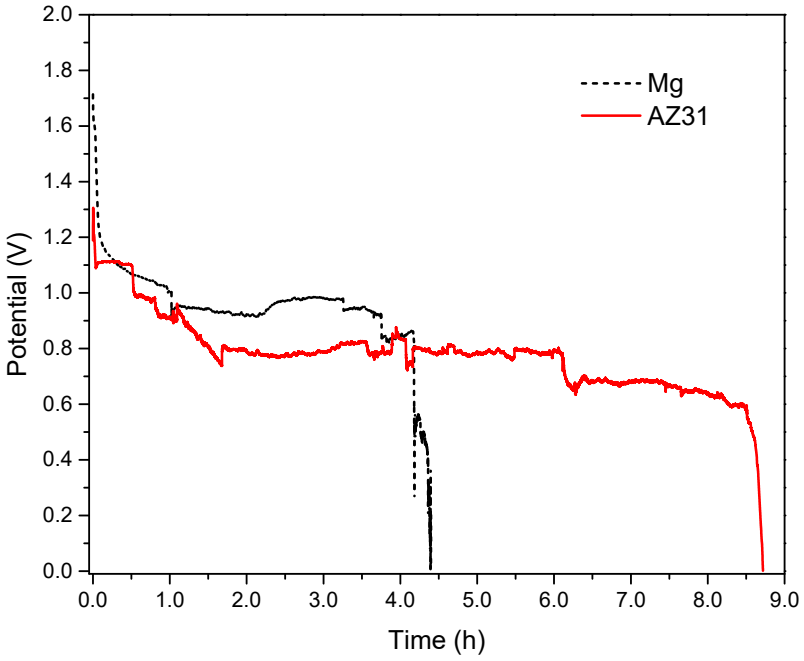

Figure 2: Discharge profile of Mg and AZ31-based cells in seawater at a constant current of 0.25 mA/cm².

From Table 1, the AZ31-based cell has shown the best performance with a capacity of 2.17 mAh/cm², a specific power of 0.19 mW/cm², and a specific energy is 1.63 J cm^{-2}. It also has an improved discharge time lasting up to 8.68 h, which is about twice as much as the life of the pristine anode.
The prominent fluctuations in the discharge profile indicate electrode interaction with ions present in the solution. The sharp decline at the end of the discharge curve suggests the shift of cathodic reaction from oxygen reduction to hydrogen evolution. Mg undergoes strong pitting corrosion accompanied by the formation of hydrogen gas. Because the life of the battery is mainly dependent on the amount of active material in the anode, after discharge a large chunk of the electrodes are left to dissolve in the electrolyte. At higher current densities of 0.50 mA/cm² and 0.75 mA/cm², both cell combinations have similar discharge behavior but with shorter discharge time as the anode is easily consumed at these conditions.

Table 1: Cell performance of Mg and AZ31-based batteries in seawater

Anode	Potential (V)	Discharge life (h)	Specific capacity (mAh/cm²)	Specific power (mW/cm²)	Specific energy (J/cm²)
Mg	1.0	4.3	1.08	0.25	1.08
AZ31	0.75	8.68	2.17	0.19	1.63

3.3 Corrosion assessment

The inherent corrosion of magnesium in aqueous solution limits the electrochemical performance of the battery. The behavior of pure Mg cell and AZ31-based cell can be observed in a Tafel plot as shown in Figure 3. The relationship between the generated current in a cell and the electrode potential of the metal allows to determine the corrosion behavior of the system. In the presence of Al and Zn alloying elements, the corrosion potential shifts to a more negative voltage from -1.15 V to -1.22 V. The corrosion properties of the two cells in seawater were collected on Table 2. AZ31 exhibited the highest polarization resistance in seawater compared to pure Mg. This implies strong corrosion resistance in the presence of alloying elements Al and Zn. Higher corrosion current in Mg-based cells shows how it is twice more susceptible to parasitic corrosion than the alloy-based anode, indicating that a more severe corrosion occurs on its surface than in AZ31-based cells.

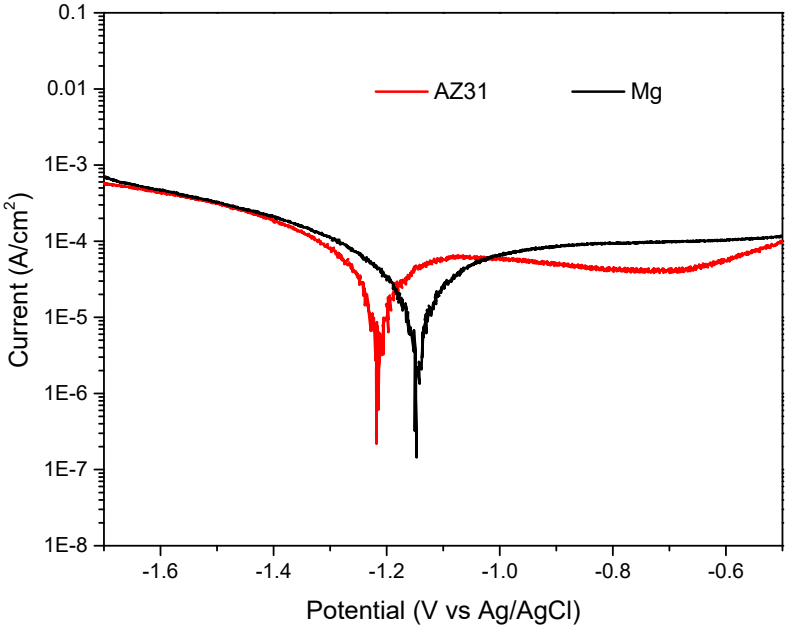

Figure 3: Corrosion behavior of Mg and AZ31-based cell in seawater

Table 2: Corrosion properties of Mg and AZ31-based cells in seawater

Anode	Corrosion potential (V vs Ag/AgCl)	Corrosion current ($\mu A/cm^2$)	Corrosion rate (mm/y^1)	Polarization resistance (Ω/cm^2)
Mg	-1.15	49.63	1.13	802
AZ31	-1.22	25.04	0.57	1,978

4. Conclusions

Material selection and optimization is the major challenge in developing a biodegradable battery. Transient battery systems composed of anodized Cu paired with two different anodes—AZ31 and pure Mg—were evaluated in a seawater electrolyte with simple nutrient. Pure Mg-based cell showed to have an operating voltage of 1.0 V lasting up to 4.3 h. When a Mg alloy AZ31 anode was used, the discharge life was significantly extended to 8.68 h, which is twice the duration of the pure Mg cell at the same discharge condition. This indicates that the presence of the alloying elements (Al, Zn) extends the life of the cell by limiting the inherent pitting corrosion of Mg. The AZ31-based battery also improved the specific energy and specific capacity of a pure Mg-based cell by 51 % and 101 %.

Fluctuations in the discharge profile can be attributed to the hydrogen gas formation. The oxide layer at the cathode provided increased supplemental sites where hydrogen can adhere. On the other hand, a highly insoluble compound, $Mg(OH)_2$ forms at the anode surface. Other than $Mg(OH)_2$, Al and Zn also accumulate at the electrode-electrolyte boundary to form the passivation layer. This limits the overall cell voltage and the useful life of the cell. One of the limitations of this study is the large mass of the electrodes left to dissolve in the electrolyte solution after discharge. Optimizing the amount of active material to completely use the bulk substance would be a good strategy for future studies.

Acknowledgments

J.M.E.A. would like to acknowledge the financial support from the Engineering Research and Development for Technology (ERDT) program of the Department of Science and Technology (DOST). J.A.D.D. would like to acknowledge Center for Advanced Batteries Program funded by Department of Science and Technology (DOST) through Niche Centers in the Regions (NICER) for Research and Development.

References

Acharya M.G., Shetty A.N., 2019, The Corrosion Behavior of AZ31 Alloy in Chloride and Sulfate Media – A Comparative Study Through Electrochemical Investigations, Journal of Magnesium and Alloys, 7(1), 98-112

Chen I. M., Phee S. J., Luo Z., Lim C. K., 2010, Personalized Biomedical Devices & Systems for Healthcare Applications, Frontiers of Mechanical Engineering, 6(1), 3–12.

Chen Y., Jamshidi R., White K., Simge C., Gallegos E., Hashemi N., Montazami R., 2016, Physical–Chemical Hybrid Transiency: A Fully Transient Li-Ion Battery Based on Insoluble Active Materials, Journal of Polymer Science, Pard B: Polymer Physics, doi: 10.1002/polb.24113.

Edupuganti V., Solanki R., 2016, Fabrication, Characterization, and Modelling of a Biodegradable Battery for Transient Electronics, Journal of Power Sources, 336, 447–454.

Hwang S. W., Tao H., Kim D. H., Cheng H., Song J. K., Rill E., Brenckle M. A., Panilaitis B., Won S. M., Kim Y. S., Song Y. M., Yu K. J., Ameen A. A., Li R., Su Y., Yang M., Kaplan D. L., Zakin M. R., Slepian M. J., Rogers J. A., 2012, A Physically Transient Form of Silicon Electronics, Science, 337(6102), 1640–1644.

Hwang S., Huang X., Seo J., Song J., Kim S., Hage-ali S., Chung H., Tao H., Omenetto F. G., Ma Z., Rogers J. A., 2013, Materials for Bioresorbable Radio Frequency Electronics, 1–6.

Jeong C., Choi C. H., 2012, Single-step Direct Fabrication of Pillar-on-pore Hybrid Nanostructures in Anodizing Aluminum for Superior Superhydrophobic Efficiency, ACS Applied Materials and Interfaces, 4(2), 842–848.

Li H., Zheng Y., Qin L., 2014, Progress of Biodegradable Metals, Progress in Natural Science: Materials International, 24(5), 414–422.

Liu T., Chen S., Cheng S., Tian J., Chang X., Yin Y., 2007, Corrosion Behavior of Super-hydrophobic Surface on Copper in Seawater, Electrochmica Acta, 52(28), 8003-8007.

Togonon J. J. H., Esparcia E. A., del Rosario J. A. D., Ocon J. D., 2021, Development of Magnesium Anode-Based Transient Primary Batteries, Chemistry Open, 10(4), 471–476.

Tsang M., Armutlulu A., Martinez A. W., Ann S., Allen B., Allen M. G., 2015, Biodegradable Magnesium/iron batteries with Polycaprolactone Encapsulation: A Microfabricated Power Source for Transient Implantable Devices, Advanced Materials, doi: 10.1002/adma.201300920 .

Xiao F., Yuan S., Liang B., Li G., Pehkonen S.O., Zhang T., 2015, Superhydrophobic CuO Nanoneedle-covered Copper Surfaces for Anticorrosion, 3(8), 4374-4388

Xin Y., Liu C., Zhang X., Tang G., Tian X., Chu P. K., 2007, Corrosion Behavior of Biomedical AZ91 Magnesium Alloy in Simulated Body Fluids, Journal of Materials Research, 22(7), 2004–2011.

Yin L., Huang X., Xu H., Zhang Y., Lam J., Cheng J., Rogers J.A., 2014, Materials, Designs, and Operational Characteristics for Fully Biodegradable Primary Batteries, Advanced Materials, 26(23, 3879-3884.

Yun Y., Dong Z., Lee N., Liu Y., Xue D., Guo X., Kuhlmann J., Doepke A., Halsall H. B., Heineman W., Sundaramurthy S., Schulz M. J., Yin Z., Shanov V., Hurd D., Nagy P., Li W., Fox C., 2009, Revolutionizing Biodegradable Metals. Materials Today, 12(10), 22–32.